PROCEEDINGS, Fifteenth Workshop on Geothermal Reservoir Engineering
Stanford University, Stanford, California, January 23-25, 1990
SGP-TR-130

STUDY OF THE EFFECT OF SEVERAL WELLBORE CONDITIONS ON THE OUTPUT CHARACTERISTICS OF WELLS AT THE ASAL FIELD, REPUBLIC OF DJIBOUTI

Battistelli, A.*, Rivera, R.J.*, Celati, R.** and Mohamed, A.***

* Aquater S.p.A., S. Lorenzo in Campo, Pesaro, Italia.
** Istituto Internazionale per le Ricerche Geotermiche, Pisa, Italia.
*** ISERST, Djibouti, Republic of Djibouti

ABSTRACT

Four deep wells were drilled in the Asal Rift Area in the Republic of Djibouti from June 1987 to July 1988 ⊙ Two of them, wells Asal 3 and Asal 6, were productive.

Well Asal 3 was extensively tested for about 4 months. Measurements taken during the long term production test showed the following features:

a) High scale buildup was observed at the surface facilities; the scaling was composed mainly of sulphides (galena and sphalerite) and amorphous silica.
b) Well output strongly decresed in time, specially at the higher flow rates range.
c) Down-hole pressure at a given flow rate decreased but the transient tests did not indicate an increase in skin factor.
d) A caliper log showed that only a limited decrease of production casing diameter occurred in the two-phase section of flow.

The contribution of various factors affecting the wellbore output was analyzed by means of a steady-state flow simulator. This simulator takes into account the high salt content of produced brine , as well as the effect of brine composition ⊙

The most important result obtained from the analysis of the contribution of several factors to the observed flowing pressure losses was that the increase in absolute scaling surface roughness, up to the point measured in the well, could be identified as the main factor affecting the output behaviour of well Asal 3; while the bottom-hole pressure drawdown and the diameter reduction played a secondary role.

On the other hand, well Asal 6 was tested for about one month. The fluid characteristics and the scaling tendency were similar to that exhibited by well Asal 3. Its output performance was mainly influenced by the presence of an obstruction located just below the production liner shoe.

The stepped well completion and the production diameter smaller than that used in the completion of well Asal 3, both determined an increase of flowing pressure losses.

Using the data obtained during production tests and the borehole flow simulator, the effect of the obstruction on downhole flowing conditions and on wellbore output was studied. An estimation of well productivity without obstruction was also performed.

MAIN CHARACTERISTICS OF WELL ASAL 3

Well Asal 3 (A3) is located on the south-western border of the Asal Rift, about 40 m far from well Asal 1 drilled in 1975 (Gringarten, 1977). As shown in Fig. 2, the well crossed a typical sequence of the Asal Rift series, formed mainly by basalts with rhyolites and interlayered sedimentary levels (Gianelli et al., 1990). This figure also illustrates the well completion.

Main permeable zones for this well are located at about 1075 m, and between 1225 and 1250 m. The temperature of produced fluids from both zones is slightly different; it is about 256°C for the upper zone and 265°C for the lower one. Static pressure is about 81 bar at a depth of 1075 m. Down-hole temperature measurements suggest that the deeper inflow may be greater than the shallow one.

ANALYSIS OF PRODUCTION DATA FROM WELL A3

Fig. 3 shows the output characteristic curve from well A3: two curves are included in this figure, curve 1 was determined after 15 to 25 days of production, whereas curve 2 was determined after 100 to 105 days. In the time comprised between these two complete determinations of the production curves a continuous decrease of output from the well was detected.

The reason of the different behaviour exhibited by well A3 during the determination

of output curves 1 and 2 mentioned above is not apparent. To find an explanation for this difference, it is necessary to take into account the contemporary change in several important parameters that could have taken place in the time transcurred between both curves. Among them: scale build-up within the wellbore, reduction in average reservoir pressure, changes in fluid thermodynamic conditions within the wellbore, and the presence of a string of drill pipes lost during the air-lift maneuver were considered. In the following paragraphs a brief description of the effect of each one of these parameters is included.

A. EFFECT OF SCALE DEPOSITS

From the study of the chemical behaviour of produced fluids (Aquater, 1989; d'Amore et al., 1990) it is believed that sulphides may start to precipitate inside the wellbore as soon as the flash occurs; meanwhile the amorphous silica phase precipitate at lower temperatures. From the analysis performed on scale samples taken from surface facilities, it was found that scale was made of sulphides (PbS and ZnS) and amorphous silica. It is believed that silica was already present at a temperature of about 220°C. These scale samples showed a high rougness with picks as high as 6 to 8 mm.

A caliper log was run at the end of the production tests, which lasted for about 130 days, by means of a mechanical tool specially designed for this purpouse. From this log a quite uniform thickness of scaling was detected from the surface down to about 800 m with thickness ranging from 7 to 10 mm. It was found that scale was absent below 850 m, which corresponds to the lower limit of the flashing zone.

Up to the time when the caliper log was run, a strong reduction of effective flow area inside the wellbore due to scale build-up was considered as a possible explanation of the observed output decline. However, from the results of the caliper, it was apparent that the measured reduction in effective area of the production casing could not explain by itself the output decline observed. Results of the combined effect of scale thickness together with other factors are discussed later.

B. EFFECT OF STRING OF DRILL PIPES

After well completion and since it was unable to start producing by itself, air-lift induction was performed. At the end of the maneuver a string of about 90 m of 4 1/2" drill pipe was lost, remaining inside the well during all production tests.

Although a decrease in output capacity from the well could be expected due to the presence downhole of the additional restriction of the drill pipe, it is believed that since it was always present during the whole productive history of the well, it could not produce by itself the output decline previously described, unless it could be combined with the simultaneous effect of other factors.

The top of the drilling string was detected at a depth of about 1190 m. It always remained within the single-phase flow section of the well, down below the flashing zone; therefore, no scale build-up could be expected at the drilling string. On the other hand, although the presence of some wall collapse below 1190 could not be completely excluded, it seems unlikely since no increase in skin factor or decrease in productivity index was detected from well tests performed at different times (Aquater, 1989). In addition to this, the contribution to total output coming from the deeper zone located below 1225 m was apparent, as evidentiated by an increase in flowing temperature from about 262 to 264 °C. Taking into account all these facts, it seems unlikely that the observed decline of well output in time could be associated with the downhole presence of the drilling string.

C. EFFECT OF AVERAGE RESERVOIR PRESSURE

Fig. 4 shows measured flowing downhole pressure at a reference depth of 1075 m. Data are plotted as a function of mass flow rate. As it can be seen from this figure, two linear relationships can be associated with the data points. Curve A fits data collected up to the time when the first output curve was measured, while curve B is based upon data collected at different times in the period between the two curves, when the well produced at a higher flow rate. This behaviour suggests a decrease in the average reservoir pressure but seems to exclude important changes in the productivity index of the well. As it will be shown later, the observed decrease in average reservoir can not by itself explain the observed output decline.

D. EFFECT OF CHANGES IN FLUID THERMODYNAMICS WITHIN THE WELLBORE

To study the combined effect of changes in fluid thermodynamic conditions within the wellbore, coupled with other factors, a computer model was used to analyze the production data from Asal wells.

a) Brief Description of the model

This computer code was written taking as a basis the approach previously presented by Barelli et al., (1982). Shortly, the model solves the problem of two-phase flow in a vertical pipe, taking at the same time into account the thermodynamic behaviour and mass

tranfer between the phases of the rising fluid. The latter is accomplished by means of the simultaneous solution of the mass energy and momentum equations. In this scheme the temperature is chosen as the governing parameter, whereas an iterative procedure is made on the energy equation.

The model account for the presence of dissolved salts in the liquid phase as well as the presence of non-condensable gases, which are considered as being made of CO_2. Main equations are as follows: (1)

1) Mass balances:

a) Brine (water + salt):

$$W_t = W_l + W_g = W_l + W_t\, x \qquad (1)$$

where x is the steam quality.

b) Carbon dioxide:

$$C_t = C_l + C_g = C_l + C_t y \qquad (2)$$

where y is the carbon dioxide quality.

2) Momentum balance:

$$(P_o - P)\,/\Delta Z = \tau_{fr} + \tau_{ac} + \tau_{gr} \qquad (3)$$

3) Energy balance:

$$h_o = h + q + \Delta E_k + \Delta E_p \qquad (4)$$

An expression for the global pressure gradient is considered, without refering to the flow regime in the wellbore. The experimental correlation was originally presented by Lombardi et al. (1978) and Bonfanti et al. (1979) from the Italian Institute CISE. This correlation can be expressed in the following way:

$$\tau_{fr} + \tau_{gr} + \tau_{ac} = \frac{2G_T^{\,2}\,(f_L\, b_L + f_G\, b_G + f_m\, b_m)}{A_f^{\,2}\, D\varrho_m} + \varrho_m\, g + \frac{G_T^{\,2}\,\Delta(1/\varrho_m)}{A_f^{\,2}\,\Delta z} \qquad (5)$$

where the flow-rate density is defined as

$$\varrho_m = G_T/Q_T \qquad (6)$$

and the friction factors for liquid, f_L, and gas, f_G are determined as functions of the Reynolds number by means of Colebrook's equation. The mixture friction factor, f_m, is a function of a dimensionless parameter which depends on the physical properties of both the fluid and the system.

Parameters b_L, b_G and b_m are function of steam quality, x, and were determined from experimental data fitting. This correlation was previously checked by Barelli (1982) under different conditions of salinity, gas concentration, pressure, temperature and enthalpy.

Mainly because of the high salinity exhibited by Asal brines (about 116 000 ppm total dissolved solids), several modifications were introduced in the routines which calculate thermodinamical properties.

Saturation brine enthalpy was calculated from data presented by Phillips et al., (1981), accounting for the contribution of CO_2 enthalpy. For this purpouse the approach of Sutton (1976) was followed. To calculate the Henry constant for dissolved CO_2 in pure water and sodium chloride brines, the salting out concept was used, together with the data presented by Cramer (1982).

b) Model calibration

Fig. 5 shows measured pressure and temperature data, as well as the theoretical fluid behaviour calculated by means of the numerical model, given by curve A. To calculate the sodium chloride concentration equivalent to the total chloride content, the composition of the Asal 3 brine at reservoir conditions was used. Table 1 below shows the main components of this brine.

Table 1 - Main components of the Asal brine

Element	ppm	molal concentration
Cl^-	70 058	1.976
Na^+	24 865	1.082
K^+	4 826	.123
Ca^{++}	15 879	.396
Total conc.	115 628	

Using the concentrations shown in Table 1 above, an equivalente NaCl concentration of 115 450 ppm was calculated. As it can be observed, this calculated value is very close to the total concentration of the main salts present.

By using the equivalent NaCl concentration mentioned above, it was observed that the model calculated a theoretical pressure vs. temperature curve, given by curve A in Fig. 5, which was different from that actually followed by the fluid. Taking into consideration that about 32 percent of salt concentration by molality is represented by KCl and $CaCl_2$ salts, it was concluded that it

(1) Nomenclature and References are given at the end of paper.

was not possible to properly represent the behaviour of a "complex brine" by the simplifying assumptions involved in the usual calculation of an equivalent NaCl composition. In addition, it should be recognized that the observed departure of the calculated vapor pressure curve also could be due to a combined effect of all thermodynamic variables involved in its determination.

Therefore considering also the total high salinity of Asal brine, it was attempted to simulate the behaviour of this "complex brine" by means of simple approach. The calculation of vapor pressure was made by using NaCl concentrations higher than the equivalent salinity previously calculated until a satisfactory match was obtained. This satisfactory agreement was obtained with an equivalent NaCl concentration of about 160 000 ppm, as shown by curve B on Fig. 5.

Other fluid properties were calculated based upon the originally calcultated equivalent salinity value.

In the following paragraphs analyses are made of changes of fluid thermodynamics within the wellbore produced by several factors.

EFFECT OF DIFFERENT PARAMETERS ON THE PRODUCTION DECLINE OF WELL A3

The computer model described before was used to study the effect on the production decline of the well of all factors already mentioned.

As previously stated, produced brine showed a strong scaling tendency. Once salt precipitation started inside the wellbore, an increase in scale thickness with production time should be expected. Therefore, it was necessary to estimate the scale growth rate to be able to describe the reduction in time of the producing casing area available to flow. Based upon results previously mentioned from the caliper log, on the scale thickness present at the end of the production period and assuming that the scale volume was a linear function of cumulative production, a scale rate of about 1×10^{-8} ($m^3\ kg^{-1}$) was determined. This value of scale deposition rate would generate a reduction in the production casing diameter from its initial value of 222 mm to a value of 220 mm during the first output curve, and to 208 mm during the second one. For modelization purpouse this scale was considered as a constant thickness layer on the casing wall extending from the surface down to 820 m. This distribution of the scale deposits agrees with that observed, eventhough its thickness was not actually constant.

On the other hand, it was attempted to obtain a reliable model for the variation of scaling surface roughness with depth; however, no direct observations were available and the approximation of a constant value at any depth proved to be incorrect.

MATCHING OF DYNAMIC PROFILES

The computer model previously described was used to match measured dynamic pressure and temperature (P/T) profiles run under several flowing conditions. Fig. 6 shows measured P/T profiles at a flow rate of about 222 t/h, run during the first output curve. Measured values were 72.7 bar and 262°C for flowing pressure and temperature, respectively, at a depth of 1075 m. As it can be observed from this figure, a good match for both curves was obtained. For this match two zones with different roughness were assumed, one with a roughness (e) of 1.8×10^{-4} m extending from the surface down to 400 m, and a second one with $e=0.5 \times 10^{-4}$ m extending from 400 down to 820 m. As previously mentioned, a good match was not obtained with a scale layer having a uniform roughness value.

A sensitivity study was performed changing several parameters and comparing the results with measured values. Table 2 summarizes results from this study. The effect on calculated wellhead pressure induced by changes in flowing down-hole pressure (FDHP), at a reference depth of 1075 m, flowing temperature at the same depth (FDHT), casing internal flowing effective diameter, and scale roughness were determined.

As a basis for the sensitivity study, P/T profiles measured during the second output curve were used. These profiles were measured under a flow rate of about 194 t/h. Fig. 7 shows measured points, as well as computed profiles for cases 3 and 4 mentioned in Table 2, above.

Case 1 illustrates the effect of a change in FDHP. For this purpouse, let's assume that all parameters, but the FDHP, remained the same as those used to obtain the match of the P/T profiles illustrated in Fig. 6, which correspond to conditions prevailing during the first output curve. As is evident from Table 2, the calculated wellhead pressure (WHP) when the FDHP is changed to that actually measured, is too high respect to the measured one. Now, let's go formard one more step and assume that not only the FDHP had changed, but also the casing ID has now the value measured after the second output curve, as shown by case 2 in Table 2 above. Although a decrease in calculated WHP is observed, it is still too high respect to the value measured.

Case 3 in Table 2 above shows the result obtained when in addition to FDHP and ID casing, the actually measured FDHT is considered. As it can be seen, even now the calculated WHP is still too high. The next

step was to change the scale roughness, keeping all other parameters constant, until a good match with the observed WHP was obtained. This is illustrated as case 4 in Table 2 and Fig. 7.

As it can be concluded from the results of the sensitivity analysis shown in Table 2, increases in scale roughness seems to be the dominant factor in explaining the observed decrease in WHP, since the combined effect of changes in both FDHT and casing ID produced a decrease of only 0.16 bar in WHP for the case under study. To further support this conclusion, a more detailed sensitivity study of the effect of changes in FDHP was performed. For this purpouse, calculations of case 1 were repeated, changing the FDHP, starting from 61 up to 74.5 bar. Comparing the results obtained to the value actually measured, it was determined that for any value of FDHP departing from the measured one, only about 20 percent of this difference could actually be transmitted to wellhead, confirming the conclusions previously discussed. Therefore, it can be concluded that for the amount of scale present in the well at the time of testing, the observed output reduction could be attributed to high pressure losses within the high flow rate range, experienced in the two-phase section of the well mainly due to scale roughness.

It must be pointed out that scale roughness values reported in Table 2 do not represent the actual height of scale picks, but they only correspond to average values used by the model, that produced friction losses equal to those experienced in the field.

THEORETICAL ANALYSIS OF DIFFERENT WELL COMPLETIONS

To perform a preliminary analysis on the effect of different well completion designs on the discharge behaviour of well A3, a simulation of theoretical output curves for three different well completions was performed. Completions under consideration were the following:

Case A: 9 5/8" casing set at 1016 m (actual completion);
Case B: 13 3/8" casing at 400 m and a 9 5/8" liner from 380 m to 1016 m (stepped completion);
Case C: 13 3/8" casing set at 1016 m.

Results obtained for the three cases are shown in Fig. 8. These results should be considered as preliminary from which guidelines can be withdrawn for further research. It was assumed that the reservoir could supply enough fluid to support the flow rates required in all cases.

Static pressure at 1075 m was 81 bar whereas the pressure drawdown was calculated with a productivity index of 29.8 t/h bar^{-1}. In all cases the scaling thickness and roughness correspond to the second output curve conditions. From Fig. 8 it can be seen that flow collapse takes place at higher flow rates in going from cases A through C.

The increase in flow rates obtained for cases B and C suggests that for a well exhibiting a high productivity index like well A3, the diameter of the production casing is a limiting factor to wellbore deliverability. On the other hand, benefits of production diameter increase are more evident in the high WHP range, becoming stable as the WHP decreases. Under these conditions the high fluid velocity has a greater effect, since it produces large friction losses in the upper part of the well due to pipe roughness.

For case B a carefull evaluation of the scale deposition rate should be made. Scale deposition could become critical at the liner top, where the enlargement from 9 5/8" to 13 3/8" is present.

Case C would seem to offer the most attractive solution as far as obtaining a larger output for a given WHP is concern; however, practical problems of drilling a well with this completion in the Asal area are present. On the other hand, it should be considered that the minimum flow rate to sustain a stable flow is high and there is the possibility that a low productivity well could not be able to sustain it.

WELL ASAL 6

Well Asal 6 (A6) was drilled 300 m NW of well A3, reaching a final depth of 1761 m. The stratigraphic column closely conforms to that of well A3. Static temperature and pressure are also very similar to those measured in A3. On the other hand, because of drilling problems, well A6 has a different completion: the 9 5/8" casing was set at 388 m and a 7" liner from 364 m to 919 m.

Fig. 9 shows the output curve from this well, determined through a production period that lasted 25 days. After production started, the presence of an obstruction of unknown nature was detected just below the 7" liner shoe, making impossible to run any instrument below this depth.

The wellbore model previously described was used to match downhole measurements. In addition, an attempt was made to estimate the output from the well if no obstruction would be present, as well as that corresponding to a well completion design similar to that of A3. To perform this task, it was assumed that the main effect of the downhole obstruction could be simulated by means of a dynamic pressure drop proportional to the square of

the volumetric flow rate. Fig. 10 shows data of FDHP at a reference depth of 920 m for different mass flow rate conditions. These data could be fitted by a relationship of the form:

$$P(W_t) = P(0) - K_v W_t - K_t W_t^2 \quad (7)$$

where the laminar and turbulent pressure drop factors, K_v and K_t, respectively, were determined through a fitting routine of the data included in Fig. 10. It was assumed that the quadratic term can be associated with the concentrated pressure drop at the obstruction, considered to be proportional to the square of volumetric flow rate. It was found that for flow rates up to about 85 t/h the flash zone was located above 920 m. Fig. 10 shows that the quadratic equation seems to adjust well up to about 110 t/h.

Fig. 11 shows the matching of a dynamic pressure profile recorded at about 108 t/h and the corresponding calculated temperature profile. Curves A represent the best match obtained, while curves B show the calculated profile if no scale was present. As it can be seen, because of short production period, the scale effect is small. A caliper log run in the 9 5/8" casing after completion of the production test confirmed this result. Curve C represents the theoretical pressure profile in the well if no obstruction was present. From this analysis, it is quite evident the importance of the obstruction in the determination of the measured output curve.

The theoretical output curve without the obstruction, simulated with the numerical model is shown in Fig. 12 as curve B. Curve A represents the measured output curve, whereas curve C is the theoretical output of well A6 with a 9 5/8" production casing.

The comparison of these curves suggests that two main factors are responsible for the low productivity exhibited by the well, the presence of the obstruction, and the stepped design with a 7" liner.

CONCLUSIONS

Based upon results obtained from the studies performed with the wellbore flow simulator, as well as physical measurements made, the following conclusions can be withdrawn:

1. Although produced brine from A3 showed a strong scaling tendency on surface production lines, the magnitude of the scale build-up within the wellbore could not produce by itself the strong observed decline in well output.

2. The combined effect of a decline in average reservoir pressure, decrease in effective-to-flow inside casing area, and changes in down-hole flowing temperature could not produce a decrease in wellhead pressure as high as that actually observed.

3. The vapor pressure curve for the complex brine found in the Asal Rift resource can not be properly described by means of a brine with a standard equivalent NaCl concentration.

4. From all factors studied, pressure losses in the two-phase section of well A3 in the high flow rates range, due to increases in scale roughness could be identified as the main factor affecting the output from the well.

5. A useful first preliminary analysis on the effect of different completions on well productivity can be performed by means of the wellbore simulator, in order to define the alternative most suitable for a given condition.

6. The effect of a downhole physical obstruction other than scale on well A6 productivity was studied. It was found that the main effect of this obstruction could be simulated by means of a dynamic pressure drop proportional to the square of the flow rate.

NOMENCLATURE

A_f	flow section, m^2
b	weighting function of friction factors
C	mass flow rate of CO_2, kg s^{-1}
D	Pipe diameter, m
E_k	kinetic energy per unit mass of fluid, J kg^{-1}
E_p	potential energy per unit mass of fluid, J kg^{-1}
f	friction factor
G	Mass flow rate of fluid, kg s^{-1}
g	gravity acceleration, m s^{-1}
h	enthalpy per unit mass of fluid, J kg^{-1}
K_t	turbulent pressure drop factor, bar $(t/h)^{-2}$
K_v	laminar pressure drop factor, bar $(t/h)^{-1}$
P	pressure, Pa
Q	volumetric flow rate of fluid, m^3 s^{-1}
q	heat exchanged with rocks, J kg^{-1}
W	mass flow rate of water, kg s^{-1}
W_t	total mass flow rate, t/h
X	steam quality
Y	CO_2 quality
Z	depth, m
Δ	finite variation of
ϱ_m	mixture density, kg m^{-3}
τ_{ac}	acceleration gradient, Pa m^{-1}
τ_{fr}	friction loss gradient, Pa m^{-1}
τ_{gr}	gravitational gradient, Pa m^{-1}

REFERENCES

Aquater, (1989), "Djibouti Geothermal Project, Final Report", Governement of

Djibouti, ISERST, unpublished report.

Barelli, A., Corsi R., Del Pizzo G. and Scali C., (1982), "A Two-Phase Flow Model for Geothermal Wells in the presence of non-condensable Gas", Geothermics, Vol. 11, No. 3, 175-191.

Barelli, A., (1983), "Erratum", Geothermics, Vol. 12, No. 4, 351.

Bonfanti, F., Ceresa, I. and Lombardi, C., (1979), "Two-phase pressure drops in the low flow rate region", Energia Nucleare, 26, 841-492.

Cramer, S.D., (1982), "The Solubility of Methane, Carbon Dioxide and Oxjgen in Brines from 0° to 300°C", U.S. Bureau of Mines, Report N. 8706.

D'Amore, F., Giusti, D. and Luzi, C., (1990), "Fluid geochemistry applied to Geothermal Wells Asal 3 and Asal 6, Republic of Djibouti", under preparation, to be published on Geothermics.

Ellis, A.J. and Goulding, R.M., (1963), "The solubility of carbon dioxide above 100°C in water and in sodium chloride solutions", Am. J. of Sci., 261, 47-60.

Gianelli, G., Passerini, P., Troisi, C., Zan, L., Gaffaneh, A.E. and Haga, A.O,(1990), "Stratigraphy, authigenic mineral assemblages and temperatures of six deep geothermal wells in Djibouti with structural data on the Asal Rift"., Geothermics, in press.

Gringarten, A.C., (1978)," Well Testing in two-phase geothermal wells", paper SPE 7480.

Lombardi, C. and Ceresa, I., (1978),"A generalized pressure drop correlation in two-phase flow", Energia Nucl. 25, 181-198.

Phillips, S.L., Igbene, A., Fair, J.A., Ozbek H. and Takana M., (1981), "A Technical Databook for Geothermal Energy Utilization", LBL - 12810, UC-66a.

Sutton, F.M., (1979), " Pressure - temperature curves for a two-phase mixture of water and carbon-dioxide" , N. Zealand J. of Sci., Vol. 19, 197-301.

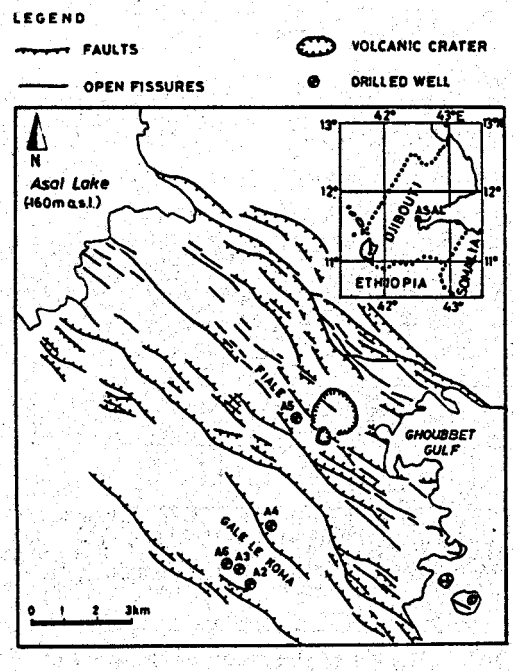

FIG.1 Structural sketch map of Asal area and location of wells drilled (after Gianelli et al., 1990)

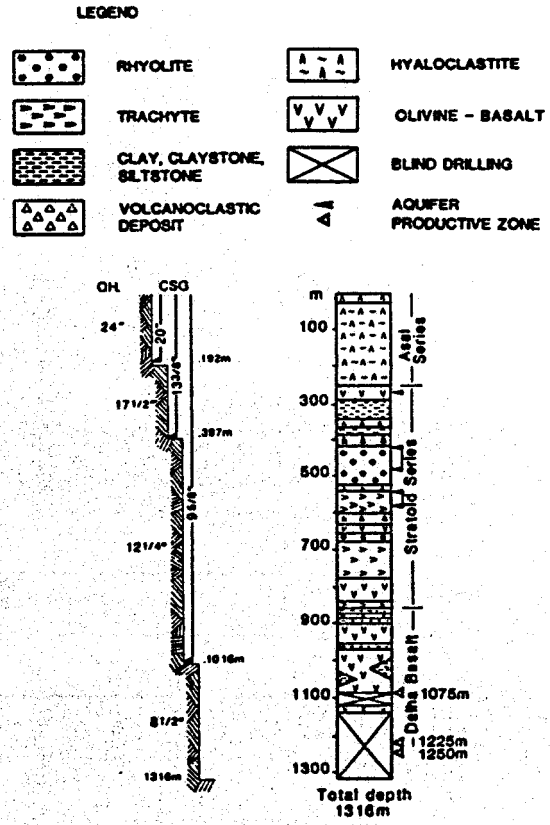

FIG.2 Stratigraphic column and technical profile of well A3. (after Gianelli et al., 1990)

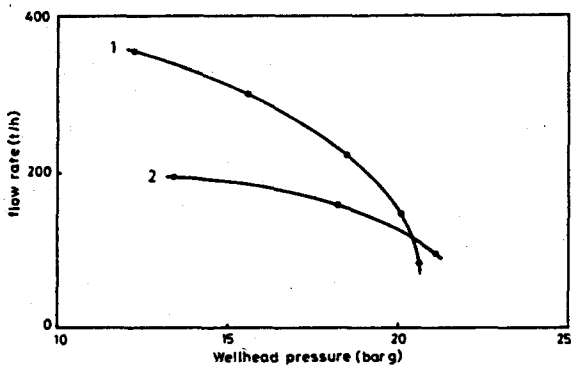

FIG.3 Output characteristic curve (O.C.C.) of well A3: (1) first O.C.C. (2) second (O.C.C.)

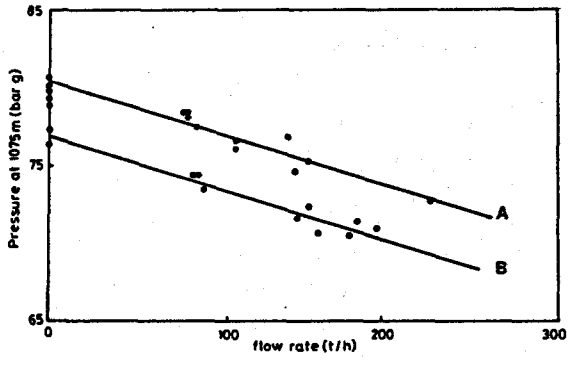

FIG.4 Bottom-hole flowing pressure at 1075 m vs mass flow rate at several times during production tests

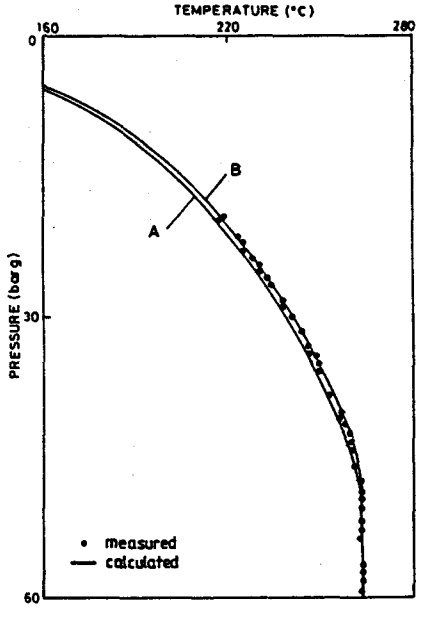

FIG.5 Measured pressure-temperature data compared with calculated thermodynamical behaviour at different sodium chloride concentrations

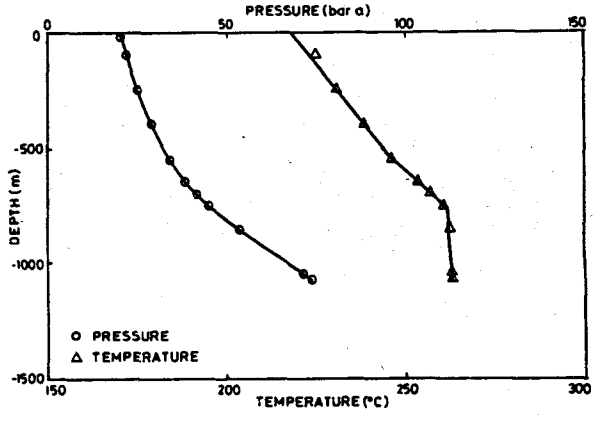

FIG.6 Measured and calculated P/T profiles at a flow rate of 222 t/h (first output curve)

Table 2 - Summary of results from the sensitivity study.

Case No.	FDHP*, bar	FDHT*, °C	Effective casing ID, m	scale roughness, m	Wellhead pressure, bar	
					calculated	Measured
1	71.6**	262	0.220	1.8×10^{-4} (1) 0.5×10^{-4} (2)	19.06	13.4
2	71.6**	262	0.208	1.8×10^{-4} (1) 0.5×10^{-4} (2)	18.45	13.4
3	71.6**	263.9**	0.208	1.8×10^{-4} (1) 0.5×10^{-4} (2)	18.90	13.4
4	71.6**	263.9**	0.208	3.4×10^{-3} (1) 0.2×10^{-3} (2)	13.50	13.4

* At a reference depth of 1075 m
** measured value
(1) From 0 down to 400 m
(2) From 400 down to 820 m

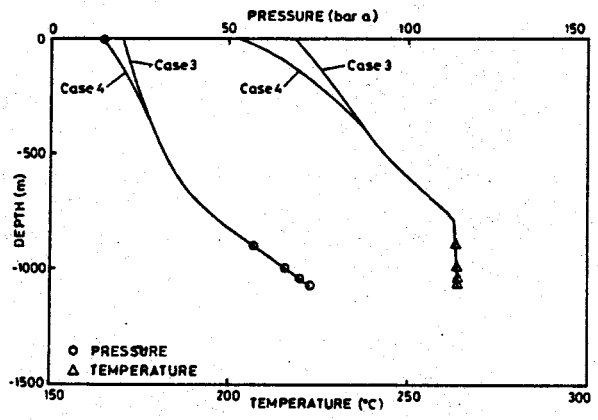

FIG.7 Measured and calculated P/T profiles at a flow rate of 194 t/h (second output curve)

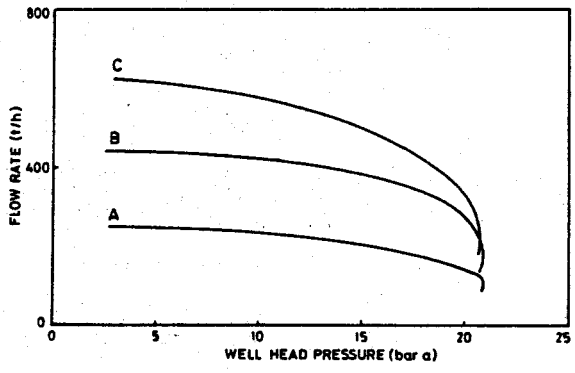

FIG.8 Computed output curves for different casing designs of well A3

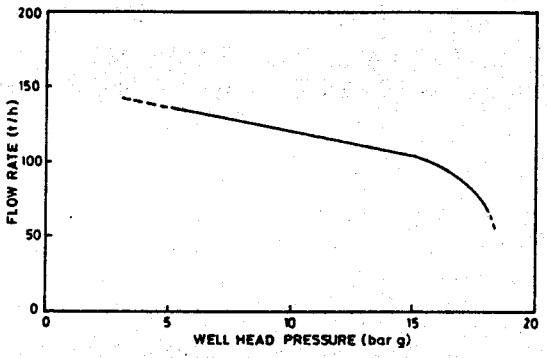

FIG.9 Measured output characteristic curve of well A6

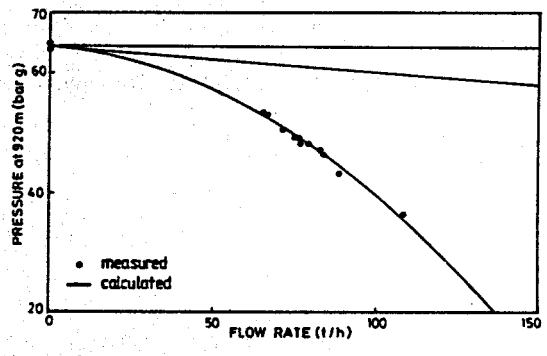

FIG.10 Pressure measured at 920 m vs mass flow rate fitted using a quadratic equation

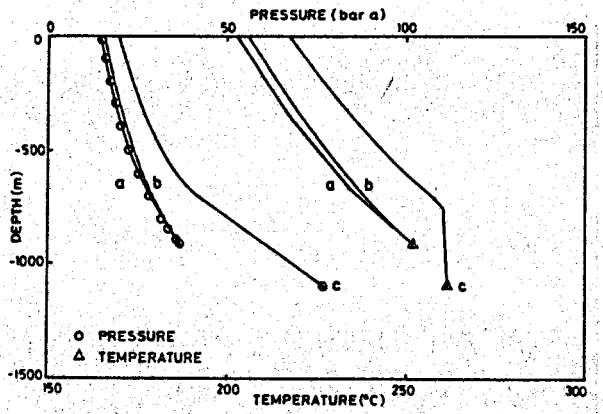

FIG.11 Measured and calculated pressure profile at a flow rate of 108 t/h

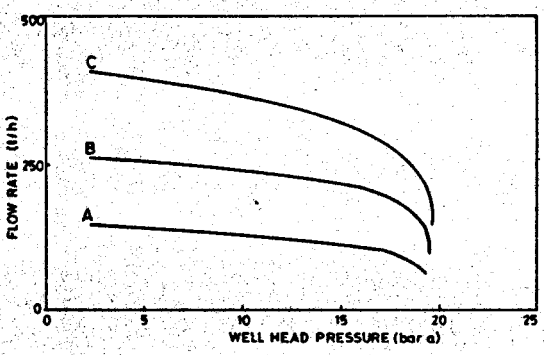

FIG.12 Measured output curve (A) of well A6 compared with the calculated curve without the obstruction (B) and with a 9 5/8" casing (C)